Available online at www.sciencedirect.com
SCIENCE DIRECT®
Tetrahedron
Tetrahedron 60 (2004) 3979–3986

Assignment of absolute configuration at phosphorus of P-chiral diastereomers of deoxyribonucleoside methanephosphonamidates by means of NMR spectroscopy☆,☆☆

Sebastian Olejniczak,[a] Milena Sobczak,[b] Marek J. Potrzebowski,[a] Matjaž Polak,[c] Janez Plavec[c] and Barbara Nawrot[b,*]

[a]*Department of Structural Studies and NMR Laboratory, Centre of Molecular and Macromolecular Studies, Polish Academy of Sciences, Sienkiewicza 112, 90-363 Lodz, Poland*
[b]*Department of Bioorganic Chemistry, Centre of Molecular and Macromolecular Studies, Polish Academy of Sciences, Sienkiewicza 112, 90-363 Lodz, Poland*
[c]*Slovenian NMR Center, National Institute of Chemistry, Hajdrihova 19, SI-1001 Ljubljana, Slovenia*

Received 16 December 2003; revised 19 February 2004; accepted 11 March 2004

Abstract—Recently, we have prepared a novel class of DNA analogues containing the [3′-NH–P(CH_3)(O)–O-5′] methanephosphonamidate linkage. Synthesis of such analogues requires preparation of the dinucleoside methanephosphonamidates N×N, where N is a 2′-deoxyribonucleoside moiety and × is the methanephosphonamidate linkage. Dimers T×T and C×T were obtained in a non-stereospecific manner giving rise to a pair of P-chiral diastereomers. Such diastereomers were effectively separated into fast and slow migrating ones by means of chromatographic methods (TLC). As described in our previous work (Nawrot et al. *Nucleic Acids Res.* **1998**, *26*, 2650), the stereochemistry of the phosphorus chiral center of T×T fast migrating diastereomer is R_P and of T×T slow migrating diastereomer is S_P, as established by means of 2D ROESY experiments. Here we describe assignment of the absolute configuration at the phosphorus center of fast and slow migrating diastereomers of C×T dimer. The 2D ROESY sequence with phosphorus decoupling during acquisition used in these measurements allowed observation of the P–Me group as a singlet instead of a $^1H-^{31}P$-coupled doublet. The apparent advantage of this approach was a much better signal to noise ratio and improved resolution in the F1 dimension. For the fast migrating C×T diastereomer an R_P and for slow migrating C×T diastereomer an S_P configuration was assigned. Conformational analysis of both pairs of diastereomers T×T and C×T indicates significant differences in sugar ring puckering, which strongly depend on the nature of the nucleobase at the 5′-terminus of the dimer. The ribose rings of the 3′-amino-2′,3′-dideoxycytidine moiety of both diastereomers of C×T adopt predominantly a C3′-*endo* (North) conformation, while thymine-substituted ribofuranoses originating either from C×T or T×T dimers prefer a C2′-*endo* (South) conformation.
© 2004 Elsevier Ltd. All rights reserved.

1. Introduction

Among the many DNA analogues considered for therapeutic applications as antisense[1] and/or antigene[2] agents, much attention has been focused on oligo(deoxyribonucleoside methanephosphonate)s with the R_P configuration.[3] Such constructs are of great interest due to their improved affinity toward double-stranded DNA, resistance to *exo*-nucleolytic degradation, enhanced cellular uptake and low affinity for proteins.[4] Oligo(nucleotide 3′-NH–P(O)O^--5′-phosphoroamidate)s, introduced by Gryaznov,[5] are second generation antisense constructs. Besides stability to phosphorodiesterases, such DNA analogues possess excellent hybridisation properties toward RNA and single- or double-stranded DNA.[6] In view of the advantageous properties of both of the above DNA analogues, we designed oligomers with the combined structural features of both classes. Thus, we synthesized thymidine dimers linked by a novel P-chiral methanephosphonamidate [3′-NH–P(O)(CH_3)O-5′] moiety and introduced them into a DNA chain in alternate positions.[7–9] Such constructs exhibit resistance to nucleolytic degradation and, for oligomers originating from fast-migrating dimers (see below), enhanced affinity toward double-stranded DNA. These features make them useful molecular tools for the inhibition of gene expression by the antigene approach (as triplex forming oligonucleotides, TFOs). In our approach to the synthesis of such oligomers we prepared dinucleoside methanephosphonamidates N×N,

☆ CDRI Communication No. 6414.

☆☆ Supplementary data associated with this article can be found in the online version, at doi: 10.1016/j.tet.2004.03.035

Keywords: Dinucleoside methanephosphonamidates; NMR structure; Conformational analysis; Molecular modelling.

* Corresponding author. Tel.: +48-42-681-6970; fax: +48-42-681-5483; e-mail address: bnawrot@bio.cbmm.lodz.pl

0040–4020/$ - see front matter © 2004 Elsevier Ltd. All rights reserved.
doi:10.1016/j.tet.2004.03.035

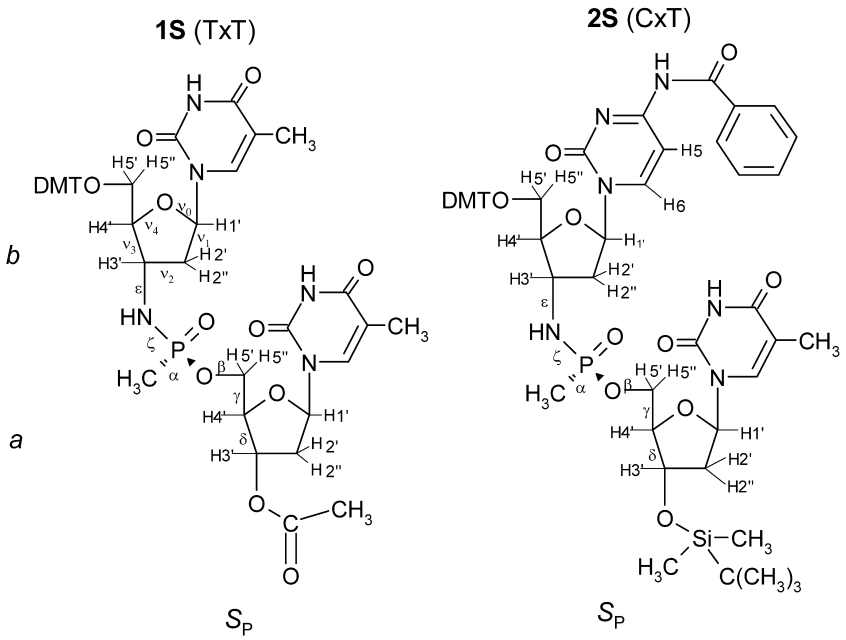

Figure 1. Schematic structures of Sp diastereomers of dimers T×T (**1S**) and C×T (**2S**) with the atom numbering and respective torsion angles. DMT is a 4,4′-dimethoxytrityl group.

Table 1. Spectral characteristics of diastereomers **F** and **S** of dimer C×T[a]

	2F		**2S**	
	b	*a*	*b*	*a*
(a) ^{1}H chemical shifts (ppm) of the ribofuranose rings of diastereomers **2** at 23 °C (*a* and *b* are as described in Figure 1, Thy is thymine and Cyt is cytosine residue)				
H1′	6.23	6.03	6.23	6.07
H2′	2.50	2.20	2.48	2.20
H2″	2.56	2.18	2.53	2.20
H3′	4.07	4.33	3.92	4.40
H4′	4.00	3.94	3.97	3.92
H5′	3.42	3.90	3.41	3.94
H5″	3.63	4.06	3.70	4.06
P–CH_3	1.33		1.30	
N–H	3.48		3.40	
$H6_{Thy}$		7.25		7.24
CH_{3Thy}		1.84		1.86
$H6_{Cyt}$	8.40		8.44	
$H5_{Cyt}$	7.20		7.28	
(b) ^{13}C chemical shifts (ppm) of diastereomers **2** from HMQC at 23 °C				
C1′	86.57	87.21	86.40	86.61
C2′	42.12	40.23	42.39	40.51
C3′	49.75	72.34	49.94	72.1
C4′	85.56	85.56	86.24	86.24
C5′	61.47	63.42	61.72	63.14
C6	145.26	137.07	144.94	113.61
C5	96.9		97.11	
CH_{3Thy}		12.61		12.82
P–CH_3	14.12		13.94	
(c) $^3J_{HH}$ coupling constants (Hz) of the ribofuranose rings of diastereomers **2F** and **2S** at 23 °C				
H1′–H2′	3.4	6.8	3.0	6.8
H1′–H2″	6.7	6.8	7.0	6.8
H2′–H3′	7.4	6.4	7.5	6.3
H2″–H3′	8.4	3.1	8.3	3.6
H2′–H2″	13.7	13.6	13.8	12.3
H3′–H4′	7.5	3.2	7.7	3.5
H4′–H5′	3.8	5.0	3.2	4.1
H4′–H5″	2.5	3.2	2.5	4.1
H5′–H5″	10.8	11.0	10.9	11.4

[a] Measurement error is ca. +/−0.2 Hz.

where N is T or dC, and × represents the methanephosphonamidate linkage.[10] As with the methanephosphonates, the non-stereospecific synthesis of the methanephosphonamidate dimers leads to a mixture of two diastereomers at phosphorus, namely S_P and R_P. Diastereomers are labelled by their silica gel mobility as fast (**F**) or slow (**S**) migrating ones. For a pair of dithymidine diastereomers T×T (**1**) an assignment of the absolute configuration at phosphorus as *R* for the fast migrating dimer (**1F**) and *S* for the slow migrating dimer (**1S**) has already been proposed on the basis of 2-D NMR ROESY experiments.[7] Here we present our study on the conformational analysis and the determination of the absolute configuration at phosphorus of the C×T diastereomers **2F** and **2S** by means of NMR spectroscopy and molecular modelling.

2. Results and discussion

2.1. Absolute configuration of methanephosphonamidate 2

The subjects of our study are the dinucleoside dimers T×T (**1**) and C×T (**2**) possessing a P-chiral methanephosphonamidate [3′-NH–P(O)(CH_3)O-5′] linkage. The structures of the S_P diastereomers of dimer T×T (**1S**) and C×T (**2S**) with the atom numbering and respective torsion angles are shown in Figure 1. The sugar ring of the 3′-terminal nucleoside is described as '*a*' and of the 5′-terminal nucleoside as '*b*'.

The full assignment of the structure of the **2F** (TLC fast migrating) and **2S** (TLC slow migrating) diastereomers in the liquid phase (chloroform solution) was carried out using 1D and 2D NMR techniques. In some experiments we have taken advantage of the Pulse Field Gradient (PFG) system in order to reduce the time of measurement and improve the quality of the spectra (e.g., reduction of T_1 noise).[11–13] The ^1H and ^{13}C chemical shifts as well as proton–proton ^3J coupling constants for **2F** and **2S** were assigned by means of $^1H-^1H$ PFG COSY, $^1H-^{13}C$ PFG HMQC and $^1H-^{13}C$ PFG HMBC experiments and are given in Table 1. The accuracy of $^3J_{HH}$ scalar coupling constants was verified by comparison of experimental and calculated ^1H NMR spectra employing the WINDAISY program (Fig. 2).[14] Selected regions of experimental spectra of diastereomers **2F** and **2S** are given in black and the respective calculated spectra are given in red. In order to simplify the analysis and simulation procedure, ^1H NMR spectra were recorded with ^{31}P decoupling.

The stereochemistry of the phosphorus chiral centers of **2F** and **2S** was established by means of 2D ROESY experiments. This approach was used previously for the assignment of absolute configuration of the dinucleoside methanephosphonates[15–18] and dithymidine methanephosphonamidates T×T (**1F** and **1S**).[7] Nuclear Overhauser effects (NOEs) between H-3′, H-4′ and H-5′ of the 2′-deoxyribose and protons of the P-methyl group were used as criteria for distinguishing between diastereomers with S_P and R_P configurations. The NOE between the P–Me and H-4′ of the 5′-terminal nucleoside was used for the determination of the R_P absolute configuration in the P–Me dimers (dinucleoside methanephosphonates).[15] The presence of a significant cross-peak between P–Me and H-3′ of the 5′-terminal nucleoside was reported to serve as a criterion for assignment of the S_P phosphorus configuration in dimeric methanephosphonates,[16] however further investigations of a variety of P–Me dimers only partially supported this assumption.[17] In some cases both diastereomers exhibit NOE cross-peaks from the P–Me to H-3′ of the 5′-terminal nucleoside.[15] For the R_P dinucleoside

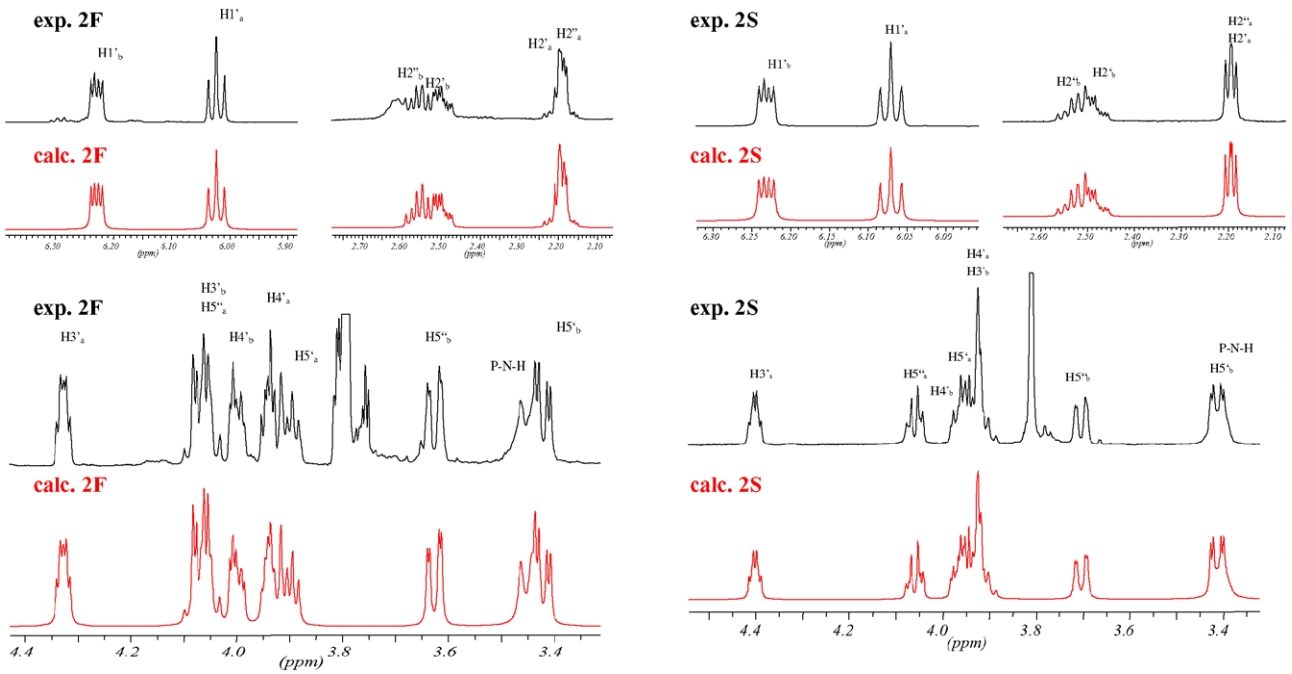

Figure 2. Comparison of experimental (500.13 MHz ^1H NMR) and calculated ^1H NMR spectra of diastereomers **2F** and **2S** employing the WINDAISY program version 940108, Bruker-Franzen Analytik. Selected regions of experimental spectra are shown in black and the respective calculated spectra are shown in red.

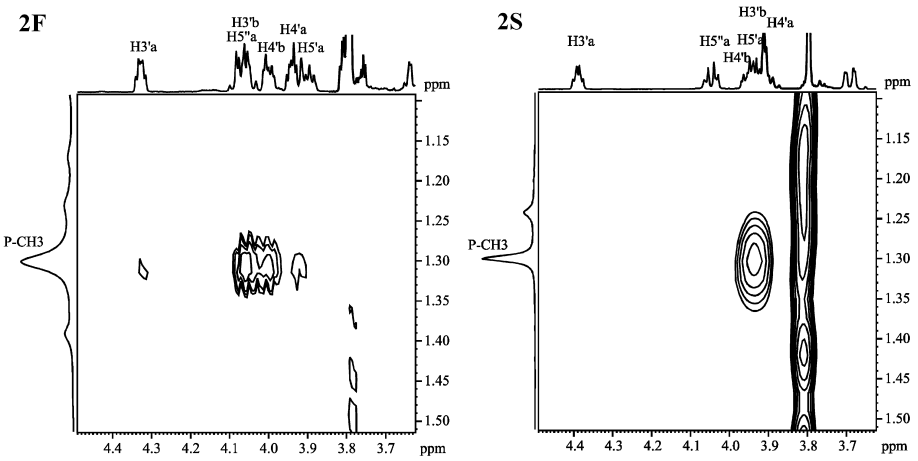

Figure 3. Selected regions of the 500.13 MHz ^{1}H NMR ROESY spectra of diastereomers **2F** and **2S**. Diagnostic cross-peaks between the *a* or *b* ribose rings protons and the protons of the P–Me group are present.

methanephosphonate NOE cross-peaks were also detected between the P–Me and H-5′ and H-5″ of the 3′-terminal nucleoside.[15] An assignment of absolute configuration at the phosphorus center in **1F** as R_P was based on the interaction between the P–Me and H-5′ of an a sugar ring.[7] Cross-peaks from the P–Me to H-4′ of the deoxyribose rings *a* and *b* were also present. A ROESY spectrum of dimer **1S** with an S_P configuration showed significant cross-peaks from the P–Me protons to H-3′ and H-4′ of the *b* deoxyribose moiety. Analogously, in the present work the most important information was obtained from inspection of cross-peaks between the P-methyl group located at the chiral centre and protons of the deoxyribose *a* and *b* rings of diastereomers **2F** and **2S**.

We used the ROESY sequence with phosphorus decoupling during acquisition. With this approach, the phosphorus-attached methyl group, which for the investigated compounds is the most diagnostic probe of stereochemistry at the phosphorus center, is observed as a singlet instead of a ^{1}H–^{31}P-coupled doublet. The apparent advantage of this approach is a much better signal to noise ratio and improved resolution in the F1 dimension. For the TLC fast migrating diastereomer C×T (**2F**) the NOE cross-peaks between the P-methyl group and protons 4′, 5′ and 5″ of the deoxyribose *a* ring as well as between protons 3′ and 4′ of the deoxyribose *b* ring are clearly separated (Fig. 3 **2F**). For the TLC slow migrating diastereomer **2S** only cross-peaks between the CH_3 and protons 3′ and 4′ of ribofuranose *b* ring are seen (Fig. 3 **2S**). Such a correlation pattern suggests an *R* configuration at the phosphorus atom of the TLC fast migrating diastereomer **2F** and an *S* configuration at P-chiral centre of the TLC slow migrating one **2S**.

Although the diagnostic NOEs of dinucleoside methanephosphonamidates are similar to those of dinucleoside methanephosphonates, in the spectra of both pairs of diastereomers, **1F** and **1S**, as well as **2F** and **2S**, there is a strong interaction between the P–Me and H-4′ of ribose *b*. This interaction may be due to the fact that the P–N bond (1.73 Å) in methanephosphonamidates is shorter than the P–O bond in the parent methanephosphonates (1.79 Å), causing decrease of the P–Me↔H-4′ of *b* interatomic distance, and thus, enhancing the NOE interaction. Molecular modelling performed previously[7] for dithymidine methanephosphonamidates **1F** and **1S** (with the help of HyperChem program, MM+ method) showed that the closest P–CH_3↔H-5′ of ribose *a* ring contact of 2.37 Å was in the structure of the R_P diastereomer. In contrast, the model structure of diastereomer S_P revealed the P–CH_3↔H-3′ of ribose *b* ring distance of 2.38 Å as the closest one. These data support our assignment of absolute configuration at the phosphorus atom as R_P for TLC fast migrating dimers **1F** and **2F** as well as S_P for TLC slow migrating dimers **1S** and **2S**.

2.2. Conformational analysis and molecular modelling of P-chiral diastereomers of dinucleoside methanephosphonamidates 1 and 2

In our previous work[7] the simple equation based on vicinal coupling constants between protons 1′ and 2′/2″[19] was used to establish population of conformers of each deoxyribose ring of **1F** and **1S**. In the present work we employed more elaborate methodology which allowed us to obtain the pseudorotation parameters. The phase angle *P*, and maximum puckering amplitude Ψ_m[20,21] for major and minor conformers were determined for the *a* and *b* sugar rings of the pairs of diastereomers **1** and **2**. In addition, these parameters were further used as constraints in molecular modelling of the most likely structure of the respective derivatives.

Conformational analysis of the sugar moiety was performed with the computer program PSEUROT[20–25] with the use of λ electronegativities[26] for the substituents along H–C–C–H fragments in the six-parameter generalized Karplus–Altona equation.[27] The vicinal coupling constants used as input were taken from the WINDAISY simulation. The following λ electronegativity values were used: 0.00 for H,

Table 2. Pseudorotational parameters of diastereomers **F** and **S** of dimers **1** and **2**. Parameters P, Ψ and $\%S$ characterize the North⇄South pseudorotational equilibrium of furanose rings *a* and *b* in each of the dinucleoside methanephosphonamidates. $^3J_{HH}$ coupling constants measurements were carried out at 23, 35 and 45 °C

Compound	Sugar	Pseudorotation parameters				% South			RMS
		P_N	$^N\Psi_m$	P_S	$^S\Psi_m$	296 K	308 K	318 K	
1F	*a*	7	30	156	30	77	78	78	0.205
	b	31	33	156	33	56	52	50	0.363
1S	*a*	37	36	196	36	81	76	76	0.065
	b	14	34	156	34	61	58	53	0.228
2F	*a*	7	29	171	29	69	68	71	0.079
	b	20	35	156	35	18	18	19	0.558
2S	*a*	16	31	171	34	65	65	64	0.051
	b	24	34	156	34	14	16	17	0.524

Pseudorotation parameters are in degrees, RMS error is in Hz.

0.58 for the heterocyclic base, 1.19 for the methanephosphonamidate [3′-NH–P(O)(CH_3)O-5′] moiety, 1.17 for OAc, 0.62 for C1′ and C4′, 0.67 for C2′, 1.40 for O4′ and 0.68 for C5′. In the optimization procedure the geometries and populations of both *N*-(C3′-*endo*) and S-type (C2′-*endo*) pseudorotamers were varied to obtain the best fit between the experimental and the calculated coupling constants. Our optimization procedure started with the following values: P_N=19°, Ψ_m^N=36°, P_S=156° and Ψ_m^S=36°. The puckering amplitude and phase angle of the minor conformer were kept frozen during individual iterative least-squares optimization, whereas parameters for the major conformer were freely optimized. The optimization resulted in the P and Ψ_m for the N- and S-type geometries of the sugar moieties which best agreed with the experimental $^3J_{HH}$ coupling constant data (Table 2).

The influence of the change of nucleobase on the conformation of the deoxyribose rings in the dinucleoside units is apparent when comparing puckering parameters for dimers **1** and **2**. The most significant distinction between dimers T×T and C×T is the conformation of the sugar rings *b* (Table 2). Conformational analysis of sugar rings in T×T (**1**) showed a preference for S-type conformers as is usual in deoxyribonucleosides and their 5′-phosphates. The comparison between *a* and *b* sugars in both slow and fast fractions of compound T×T (**1**) shows that populations of the S-type conformers in sugar ring *b* are ca. 20 unit percent lower that in the case of sugar ring *a*. It has been shown[28] that replacement of the OH group on C3′ of thymidine with an NH_2 substituent decreases the S-type population to ca. 40 percent. Thus it is reasonable to expect a lower S-type sugar population upon introduction of a methanephosphonamidate moiety as in the case of the sugar ring *b* in T×T (**1**).

In the case of compound C×T (**2**) the N⇄S pseudorotational equilibrium was biased towards S-type conformers for sugar *a* for both slow and fast fractions. For sugar *b* the N⇄S pseudorotational equilibrium was surprisingly strongly biased towards N-type conformers. Namely, the populations of S-type conformers at 296 K were 14 and 18% in **2S** and **2F**, respectively. This can be explained by two effects. First, there is a preference of the methanephosphonamidate moiety for N-type conformers, as already shown in the case of **1**. Second, there are stacking interactions of the modified cytosine bases in $CDCl_3$ that additionally drive the pseudorotational equilibrium towards the N-type conformers. Since the conformational preferences observed for 3′-substituted 3′-deoxythymidine derivatives strongly depend on the electronegativity of the 3′-substituent[28] and, as it is well known,[29] nucleoside phosphoramidates adopt predominantly a C3′-*endo* sugar ring conformation, it is reasonable to expect the methanephosphonamidate DNA analogues to adopt a North conformation for sugar rings substituted with an amino functionality that is opposite to a typical B-DNA helix ring puckering.[30] Interestingly, the chirality at phosphorus has little influence on the puckering parameters. The ratio of South to North conformers is only slightly dependent on the temperature of the experiment, resulting in subtle changes of the %S value. The biggest changes in population of the conformers as a function of the temperature are observed for sugar ring *b* of dimer **1S** [Δ(%S)=8].

Molecular modelling is an approach which allows rationalisation of constraints obtained by means of spectroscopic techniques and visualisation of the most reliable set or family of conformers. The PM3 semi-empirical method was used for calculations.[31,32] The 3D structures of **1** and **2**, calculated with partially frozen geometry, as obtained from NMR measurements, are shown in Figure 4. The calculated torsion angles which characterize chain geometry[30] and the data showing differences between energy of fully optimized and partially frozen structures of **1** and **2** are attached as Supplementary Material.

3. Conclusions

The absolute configuration at the phosphorus center of both T×T and C×T methanephosphonamidate dimers is assigned as R_P for fast migrating dimers, and as S_P for slow migrating dimers. Conformational analysis of both pairs of diastereomers indicates significant conformational differences in sugar ring puckering, which strongly depend on the nature of the nucleobase at the 5′-terminus of the dimer. The ribose rings of the 3′-amino-2′,3′-dideoxycytidine moiety of both diastereomers of C×T adopt predominantly C3′-*endo* (North) conformation, while thymine-substituted ribofuranoses in C×T or T×T dimers exist predominantly in a C2′-*endo* (South) conformation.

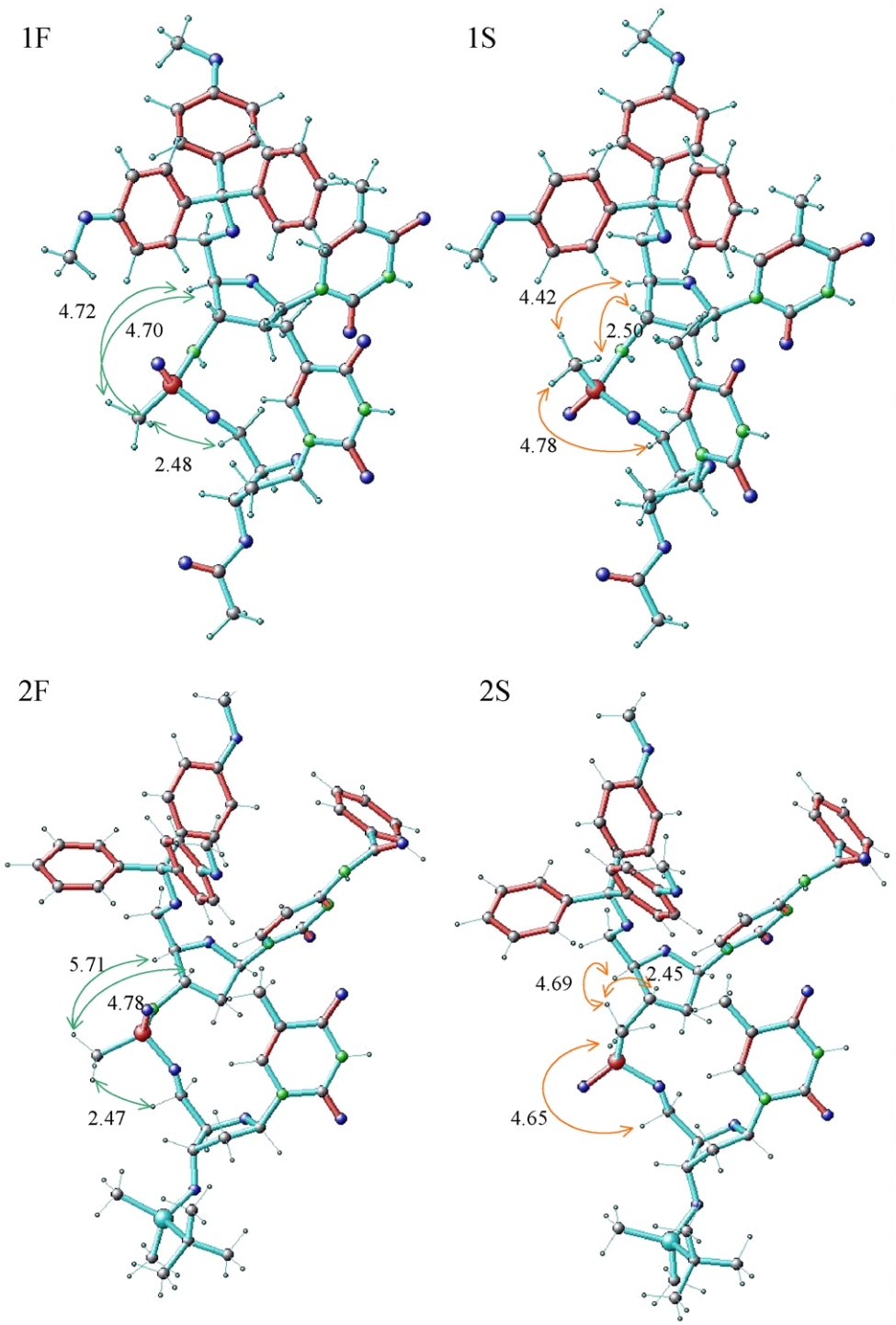

Figure 4. The 3D structures of diastereomers T×T (**1F** and **1S**) and C×T (**2F** and **2S**) obtained by means of the PM3 semi-empirical method. NOE-cross-peaks are indicated.

4. Experimental

4.1. Synthesis and purification of 2

Dinucleotide methanephosphonamidates T×T (**1**) and C×T (**2**) were synthesized and separated chromatographically into fast (**1F** and **2S**) and slow migrating diastereomers (**1F** and **2S**) as described previously.[7,10] If necessary, further purification was achieved by silica gel column chromatography in a gradient of methanol in chloroform (up to 5%). Compounds were dried in vacuo and then used for NMR measurements.

4.2. NMR measurements in the solution

The 5 mg samples of **1** or **2** were dissolved in 0.5 mL of $CDCl_3$. All spectra were recorded on Bruker Avance DRX 500 spectrometer, operating at 500.13 MHz for ^1H,

125.2578 MHz for ^{13}C and 202.46 MHz for ^{31}P. For all experiments original Bruker pulse programs were used. The chemical shift of $CDCl_3$ signal was used as a reference (δ=7.24 ppm for ^{1}H and δ=77.0 ppm for ^{13}C). 85% phosphoric acid was used as an external standard for ^{31}P spectra. The spectrometer was equipped with a Pulse Field Gradient Unit (50 G/cm). The inverse broadband probehead was used.

The COSY90 spectra were obtained from 1024 experiments with 4 scans of each. Relaxation delay was 1.5 s. The spectral width was 10 ppm (5000 Hz) in both dimensions. The data size in F2 was 4 K. Digital quadrature detection (DQD) was applied. Two 10 μs length *z*-gradient pulses, strength of about 5 G/cm each, were applied with 1 ms delay for gradient recovery. The FIDs were apodized with a sine-bell function in both dimensions. Final data were zero filled twice in both dimensions and symmetrized about the diagonal.

The ROESY spectra were recorded in a 2 K×1 K (F2×F1) data matrix. Digital quadrature detection was applied and 32 scans were accumulated in each experiment. The experiment was run in a phase sensitive mode with a 3650 ms cw pulse for the ROESY spin lock. The spectral width was 4500 Hz (9 ppm) in both dimensions. Data were processed with a sine-bell shape apodization function in both directions and TPPI in F1. No zero filling was applied.

The PFG-HMQC spectra were acquired in 1 K×4 K [F1(^{13}C)×F2(^{1}H)] data matrix. Three 1ms length z-gradient pulses, strength of about 25, 15 and 20 G/cm, in sequence were applied with 1 ms delay for gradient recovery. Spectral width was 4000 Hz (8 ppm) in F2 (^{1}H) and 25 kHz (200 ppm) in F1 (^{13}C). A Garp decoupling sequence was employed. Final data were processed with a sine function in F1 and qsine in F2 dimension.

The PFG-HMBC experiment was acquired in a 0.5 K×4 K (F1×F2) data matrix and 8 scans for each experiment. Three 1 ms length *z*-gradient pulses, strength of about 25, 15 and 20 G/cm, in sequence were applied with 50 μs delay for gradient recovery. Final data were processed with sine-bell and qsine-bell functions in F1 and F2 dimensions respectively.

4.3. Molecular modelling

All structures discussed were calculated by means of PM3 routine employing Gaussian 98 program running on the Silicon Graphic Power Challenger computer. The calculations were run until the minimum, defined by the following parameters: maximum force <0.000450; RMS force <0.000300; maximum displacement <0.001800, and RMS displacement <0.001200 was reached. Geometrical constraints were calculated for structures of compound **1** and **2** with fully optimised geometry as well with 'frozen' conformation of sugar rings as shown in Figure 4. Moreover, Figure 4 displays distances given in Å between protons for which NOE effects were observed (see Fig. 1) The data for fully optimised structures with distances between protons corresponding to those presented in Figure 4 are attached as Supplementary Material.

References and notes

1. Zamecnik, P.; Stephenson, M. L. *Proc. Natl. Acad. Sci. U.S.A.* **1978**, *75*, 280–284.
2. Giovannangeli, C.; Helene, C. *Antisense Nucleic Drug Dev.* **1997**, *7*, 413–421.
3. Reynolds, M. A.; Hogrefe, R. I.; Jaeger, J. A.; Schwartz, D. A.; Riley, T. A.; Marvin, W. B.; Daily, W. J.; Vaghefi, M. M.; Beck, T. A.; Knowles, S. K.; Klem, L. E. *Nucleic Acids Res.* **1996**, *24*, 4584–4591.
4. Crooke, S. T.; Lebleu, B. *Antisense research and application*; CRC Press: Boca Raton, FL, 1993.
5. Chen, J. K.; Schultz, R. G.; Lloyd, D. H.; Gryaznov, S. M. *Nucleic Acids Res.* **1995**, *23*, 2661–2668.
6. Gryaznov, S. M. *Biochim. Biophys. Acta* **1999**, *1489*, 131–140.
7. Nawrot, B.; Boczkowska, M.; Wojcik, M.; Sochacki, M.; Kazmierski, S.; Stec, W. J. *Nucleic Acids Res.* **1998**, *26*, 2650–2658.
8. Boczkowska, M.; Nawrot, B.; Stec, W. J. *J. Biomol. Struct. Dyn.* **1999**, *16*, 1290–1291.
9. Nawrot, B.; Sobczak, M.; Maszewska, M.; Nowak, M.; Stec, W. J. In *Frontiers in nucleic acids*; Schinazi, R. F., Liotta, D. C., Eds.; Informed Horizons, LLC: Tucker, USA, 2004.
10. Nawrot, B.; Sobczak, M.; Antoszczyk, S. *Org. Lett.* **2002**, *4*, 1799–1802.
11. Wüthrich, K. *NMR of proteins and nucleic acids*; Wiley: New York, 1986.
12. Wijmega, S. S.; Mooren, M. M. W.; Hilbers, C. W. In *NMR of nucleic acids; from spectrum to structure in NMR of macromolecules, a practical approach*; Roberts, G. C. K., Ed.; IRL: Oxford, 1993; pp 217–289.
13. Hilbers, C. W.; Wijmega, S. S. In *Encyclopedia of nuclear magnetic resonance*; Grant, D. M., Harris, R. K., Eds.; Wiley: Chichester, 1996; pp 3346–3359.
14. WINDAISY program, version 940108, Bruker-Franzen Analytik, Bremen, 1994.
15. Loschner, T.; Engels, J. W. *Nucleic Acids Res.* **1990**, *18*, 5083–5088.
16. Wang, C.; Wang, L.; Yang, X.; Jiang, T.; Zhang, L. *Nucleic Acids Res.* **1993**, *21*, 3245–3248.
17. Lebedev, A. V.; Frauendorf, A.; Vyazovkina, E. V.; Engels, J. W. *Tetrahedron* **1993**, *49*, 1043–1052.
18. Bower, M.; Summers, M. F.; Powell, C.; Shinozuka, K.; Regan, J. B.; Zon, G.; Wilson, W. D. *Nucleic Acids Res.* **1987**, *15*, 4915–4930.
19. Rinkel, L. J.; Altona, C. *J. Biomol. Struct. Dyn.* **1987**, *4*, 621–649.
20. de Leeuw, F. A. A. M.; Altona, C. *J. Chem. Soc., Perkin Trans. 2* **1982**, 375–384.
21. de Leeuw, F. A. A. M.; Altona, C. *J. Comput. Chem.* **1983**, *4*, 438–441.
22. Haasnoot, C. A. G.; de Leeuw, F. A. A. M.; de Leeuw, H. P. M.; Altona, C. *Org. Magn. Reson.* **1981**, *15*, 43–52.
23. Altona, C.; Sundaralingam, M. *J. Am. Chem. Soc.* **1972**, *94*, 8205–8212.
24. Altona, C. *Rec. Trav. Chim. Pays-Bas* **1982**, *101*, 413–423.
25. Haasnoot, C.; de Leeuw, F. A. A. M.; Huckriede, D.; van Wijk, J.; Altona, C. PSEUROT—a program for the conformational analysis of five membered rings, version 6.0. Leiden University, Leiden, Netherlands, 1993.
26. Altona, C.; Francke, R.; de Haan, R.; Ippel, J. H.; Daalmans,

G. J.; Hoekzema, A. J. A. W.; van Wijk, J. *Magn. Reson. Chem.* **1994**, *32*, 670–678.
27. Haasnoot, C. A. G.; de Leeuw, F. A. A. M.; Altona, C. *Tetrahedron* **1980**, *36*, 2783–2792.
28. Thibaudeau, C.; Plavec, J.; Garg, N.; Papchikhin, A.; Chattopadhyaya, J. *J. Am. Chem. Soc.* **1994**, *116*, 4038–4043.
29. Ding, D.; Gryaznov, S. M.; Lloyd, D. H.; Chandrasekaran, S.; Yao, S.; Ratmeyer, L.; Pan, Y.; Wilson, W. D. *Nucleic Acids Res.* **1996**, *24*, 354–360.
30. Saenger, W. *Principles in nucleic acid structure*; Springer: New York, 1984.
31. Stewart, J. J. P. *J. Comput. Chem.* **1989**, *10*, 209–220.
32. Stewart, J. J. P. *J. Comput. Chem.* **1989**, *10*, 221–264.